Research Article

Muhammad Riza Ghulam Fahmi, Adroit T.N. Fajar, Nurliana Roslan, Leny Yuliati, Arif Fadlan, Mardi Santoso, Hendrik O. Lintang*

Fluorescence study of 5-nitroisatin Schiff base immobilized on SBA-15 for sensing Fe^{3+}

https://doi.org/10.1515/chem-2019-0053
received September 11, 2018; accepted February 12, 2019.

Abstract: *N*'-(5-nitro-2-oxoindolin-3-ylidene) thiophene-2-carbohydrazide **(NH)** was successfully synthesized as a ligand, then grafted onto the surface of mesoporous silica **SBA-15** *via* an aminopropyl bridge. The successful grafting of ligand **NH** onto the hybrid nanomaterial (**SBA-15/APTES-NH**) was confirmed by infrared spectroscopy. On excitation at 276 and 370 nm, the ligand **NH** and the hybrid nanomaterial **SBA-15/APTES-NH** showed a strong and narrow emission peak centered at 533 nm. By dispersing **SBA-15/APTES-NH** in an aqueous solution containing metal ions, the resulting solid materials showed a higher binding of **NH** sensing site to Fe^{3+} ions as compared to the others with a quench of the emission intensity up to 84%. This result showed that the hybrid nanomaterial is a potential chemosensor that requires development for the detection of metal ions.

Keywords: chemosensor; hybrid material; metal ions; SBA-15; Schiff base.

***Corresponding author: Hendrik O. Lintang,** Ma Chung Research Center for Photosynthetic Pigments, Universitas Ma Chung, Villa Puncak Tidar N-01, Malang, 65151, East Java, Indonesia; Department of Chemistry, Faculty of Science and Technology, Universitas Ma Chung, Villa Puncak Tidar N-01, Malang, 65151, East Java, Indonesia, E-mail: hendrik.lintang@machung.ac.id
Muhammad Riza Ghulam Fahmi, Adroit T.N. Fajar, Leny Yuliati: Ma Chung Research Center for Photosynthetic Pigments, Universitas Ma Chung, Villa Puncak Tidar N-01, Malang, 65151, East Java, Indonesia
Muhammad Riza Ghulam Fahmi, Arif Fadlan, Mardi Santoso: Department of Chemistry, Institut Teknologi Sepuluh Nopember, Kampus ITS Sukolilo, Surabaya, 60111, East Java, Indonesia
Nurliana Roslan: Department of Chemistry, Faculty of Science, Universiti Teknologi Malaysia, 81310 UTM Johor Bahru, Johor, Malaysia
Leny Yuliati: Department of Chemistry, Faculty of Science and Technology, Universitas Ma Chung, Villa Puncak Tidar N-01, Malang, 65151, East Java, Indonesia

1 Introduction

Amongst heavy metals, iron plays an important function in living organisms and their metabolism such as oxygen-carrying and the formation of the hemoglobin [1]. However, excessive Fe^{3+} in the human body causes various problems such as cancers and dysfunction of organs while an iron deficiency can lead to anemia [2,3]. For these reasons, detecting iron ions have been an interesting area of research. For example, several analytical techniques for detecting iron ions have been generally developed using instrumental techniques such as Voltammetry, Inductively Coupled Plasma Atomic Emission Spectrometry (ICP-AES), and Flame Atomic Absorption Spectrometry (FAAS) [4,5]. However, these techniques become inaccessible because of some inherent limitations such as being expensive, complicated sample pretreatments and due to usage of harmful solvents [2,6]. Recently, fluorescent chemosensors have significantly became an interest because these compounds or materials can be used in environmental research with high sensing capabilities such as easy detection, quick response, good selectivity, high sensitivity, and low costs [7,8].

Schiff base derivatives have played an important role as a chemosensor due to their chromogenic and azomethine groups [9,10]. Schiff base could be easily prepared by condensation between a primary amine and an aldehyde or a ketone group [11]. The lone pair of electrons at the cyanide and carbonyl groups provided a good possibility for chelating to transition metal ions. It is due to the formation of π electrons in the six-membered rings [12–14]. Therefore, Schiff base can be applied as a chelating agent for the detection of many metal ions. For examples, Schiff base derived from isatin has been widely reported for chemosensors such as isatin *N*-phenylsemicarbazone [15], rhodamine-isatin [16], 2',7'-diamino-2-oxo-1',4'-dihydrospiro[indoline3,4'-quinoline]-3'-carbonitriles [17], and *N*-methyl isatin [18].

Functionalized mesoporous silica has gained wide attention due to their applications such as membranes,

drug delivery, chemosensor, and biosensor [19–22]. **SBA-15**, one of the mesoporous silica, is a promising material to be used as inorganic support because of the high thermal stability, large pore size and high surface area [20,23,24]. Besides that, the presence of OH groups from the silanol on the surface of **SBA-15** can be attached by various organic chromophores [25,26]. Moreover, for chemosensor applications [27–33], the regularly arranged pores in its **SBA-15** mesostructure can enhance the selectivity to particular guests like organic substance and/or metal ions [34]. For Schiff base ligands as fluorescent chemosensors in the hybrid mesoporous silica materials, several reports have been published for sensing Al^{3+} [35], Hg^{2+} [36], Pb^{2+} [37], Zn^{2+} [38–40], and Cu^{2+} ions [41–43]. In particular, Wang et al. [44] and Afshani et al. [45] have reported that the grafting of *bis*-Schiff base *N,N′*-(1,4-phenylenedimethyli-dyne)bis(1,4-benzenediamine) (PMBA) and salicylaldehyde with **SBA-15** can be used for sensing Fe^{3+} at a less intense blue-emission peak of the binding site consisting of a broad peak. By using isatin-isonicotinohydrazide functionalized **SBA-15**, Lashgari et al. in 2017 [46] showed that the hybrid nanomaterial can be used as a chemosensor of the same metal ion. However, the sensing capability was only found up to 70% quenching of its less intense and broad emission peak at 420 nm. Hence, it is necessary to develop chemosensors with more bright emission especially in the area closed to near infrared so that the identification and evaluation can be easily carried out and is more sensitive. On the other hands, Schiff-base from 5-nitroisatin type fluorescent chemosensors have been rarely reported [44–46] and 2-thiophene carboxylic acid hydrazide was reported as Schiff base for the fluorescent probe of 2-hydroxy-1-naphthaldehyde in the detection of Al^{3+} ions with a broad green-emission at 476 nm [47]. To the best of our knowledge, 5-nitroisatin Schiff base immobilized on **SBA-15** hybrid nanomaterials for sensing Fe^{3+} is one of the potential chemosensor with bright fluorescence and high sensing capability. Herein, we report the first example of hybrid fluorescent chemosensors with strong and intense emission at the green-to-red (533 nm) area using **SBA-15** with a Schiff-base nitroisatin based on 2-thiophene carboxylic acid hydrazide, called as *N*'-(5-nitro-2-oxoindolin-3-ylidene) thiophene-2-carbohydrazide, for the detection of Fe^{3+} ions. In particular, the new hybrid chemosensor shows high sensing capability up to 84% with low limit of detection and high reusability.

2 Experimental

2.1 Materials and Method

The materials, 5-nitroisatin (Aldrich N17807), 2-thiophenecarboxylic acid hydrazide (Aldrich T1388), aquades, dimethyl sulfoxide anhydrous (Merck 8.02912), ethanol (Merck 1.00983), sulfuric acid, ethyl acetate, acetone, *n*-hexane, chloroform, and **SBA-15** were obtained in the previous study [48]. Infrared spectra are measured using FT-IR JASCO 6800 with ATR disc, UV-Vis spectra were measured using spectrophotometer JASCO V-760, and fluorescence analysis were measured using spectrofluorometer JASCO FP-8500ST. ^{1}H-NMR spectra were obtained at 500 MHz and ^{13}C-NMR spectra were measured at 125 MHz using JMN-ECA 500 NMR machine. DMSO-*d6* was used as an internal standard and solvent. Mass spectra were obtained using Waters LCT Premier XE instrument.

2.2 Synthesis of Schiff base

Schiff base ligand **NH** was synthesized by diluting 5-nitroisatin (0.15 g; 0.80 mmol) in 20 mL of ethanol and placed in a round bottom flask as shown in scheme 1. Three drops of sulfuric acid were added and then refluxed for 20 minutes. 2-Thiophenocarboxylic acid hydrazide (0.11 g; 0.80 mmol) in 10 mL ethanol was added to the mixture and it was refluxed further at 78°C for 2 hours (the current reaction was monitored with thin layer chromatography). The mixture was cooled to room temperature and the solvent was evaporated. The remaining solid was washed with cold ethanol (2x5 mL), dried thoroughly desiccator, and identified by FT-IR, NMR and MS spectrometers.

2.3 Synthesis of SBA-15/APTES

The mesoporous silica, **SBA-15**, was prepared in the previous study [48]. 3-Aminopropyl triethoxysilane (**APTES**) was used as the silylation reagent on the aminopropyl grafting onto **SBA-15**. Typically, one gram of **SBA-15** was mixed to **APTES** (2.2 mL) in 50 mL chloroform and then stirred at room temperature for 12 hours. After that, the mixture was filtered, washed with chloroform and dried at room temperature. The resulting white solid was characterized by using FT-IR spectrometer.

2.4 Synthesis of SBA-15/APTES-NH

For the grafting of an organic compound, **SBA-15/APTES** (200 mg) and ligand **NH** thiophene-2-carbohydrazide (57 mg) were refluxed in ethanol solution (50 mL) for 24 hours. This mixture was filtered with a Whatman paper and washed with ethanol until the filtrate did not show yellow color. The resulting yellow solid was dried at room temperature and characterized by FT-IR and fluorescent spectrometers.

2.5 Fluorescent Chemosensor of Metal Ions

Sensing properties of **SBA-15/APTES-NH** were evaluated by using the solid method. Iron ions in chloride salt ($FeCl_3$) were dissolved in water with a concentration of 50, 100, 150, and 200 mM. After that, 1 mL of Fe^{3+} ion was mixed with 5 mg of **SBA-15/APTES-NH** and sonicated for 5 minutes. The mixture was centrifuged for 15 minutes, decantated and dried at 50ºC. The resulting solid sample was measured their changes in emission and excitation by using fluorescence spectroscopy. Other metal ions such as Ca^{2+}, Co^{2+}, Cu^{2+}, Fe^{3+}, K^{+}, Mg^{2+}, Mn^{2+}, and Zn^{2+} in 100 mM were also evaluated with the same experiment procedure.

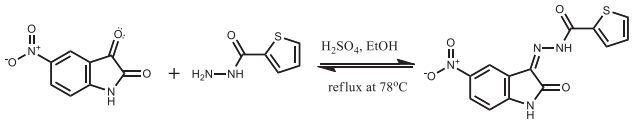

Scheme 1: Synthesis route of *N*'-(5-nitro-2-oxoindolin-3-ylidene) thiophene-2-carbohydrazide.

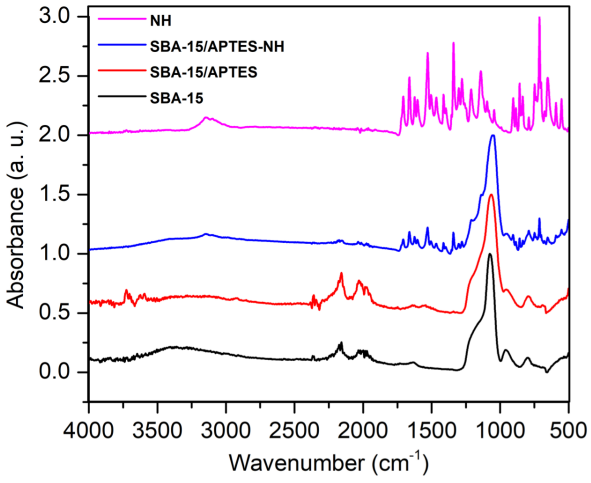

Figure 1: FT-IR spectrum of **SBA-15** (black line), **SB-15/APTES** (red line), **SBA-15/APTES-NH** (blue line) and ligand **NH** (pink line).

3 Result and Discussion

The synthesis of ligand **NH** was prepared by adapting the previous method [49]. Typically, as shown in Scheme 1, 5-nitroisatin was refluxed with 2-thiophenocarboxylic hydrazide in ethanol under acidic conditions using sulfuric acid to give ligand **NH** in 92% yield. Figure 1 shows the FT-IR spectrum of the ligand **NH**, **SBA-15, SBA-15/APTES** and the hybrid materials **SBA-15/APTES-NH**. The vibration peaks at 3149 and 1529 cm^{-1} were assigned to N-H and C=N functional groups, indicating the formation of Schiff base as the ligand **NH**. Other important vibration peaks of the ligand **NH** were identified at 1662 and 1340 cm^{-1} for carbonyl (C=O) and C=C aromatic groups. Moreover, the ^{1}H-NMR spectrum shows a singlet signal of NH hydrazide proton at chemical shift (δ) of 13.12 ppm and NH isatin proton at δ of 11.93 ppm. In addition, aromatic protons have shown their signals at δ of 7.15, 7.31, 7.97, 8.10, 8.29 and 8.30 ppm with a number of protons for 6H from isatin and thiophene rings. Mass spectrum shows the molecular ion peaks $[M+H]^+$ at *m/z* 317.3164 Da and $[M+Na]^+$ at *m/z* 339.3615 Da. The calculation of exact mass for ligand **NH** shows the molecular ion peaks $[M+H]^+$ at *m/z* 317.3000 Da and $[M+Na]^+$ at *m/z* 339.2818 Da that are closed to the observed ones. These results confirm that the ligand **NH** has been successfully formed.

In the synthesis of hybrid nanomaterial, the unmodified **SBA-15** was firstly characterized using FT-IR spectrometer. It showed the vibration bands at 3300-3750, 1080, 970-950 and 461 cm^{-1} for OH, Si–O–Si, Si–OH, and Si–O, respectively. When compared with **SBA-15**, the intensity of silanol groups at 3467 cm^{-1} was decreased in **SBA-15/APTES** concomitant with increasing intensity of N-H bands of the **APTES** aminopropyl groups. Besides that, the presence of original vibration bands in the range of 2881–2990 cm^{-1} for stretching of methylene vibrations from the propyl chain were still observed, indicating the successful grafting of **APTES** with **SBA-15** to give **SBA-15/APTES**. Moreover, since the characteristics of vibration peaks for ligand **NH** and **SBA-15/APTES** were still observed, the ligand **NH** was successfully grafted onto the surface of **SBA-15/APTES** to give **SBA-15/APTES-NH**.

Figure 2 shows the fluorescent studies of ligand **NH** and hybrid material **SBA-15/APTES-NH**. The fluorescence of these hybrid materials appears at a definite excitation wavelength because the ligand **NH** can produce strong fluorescence. Commonly, **SBA-15** did not show fluorescence

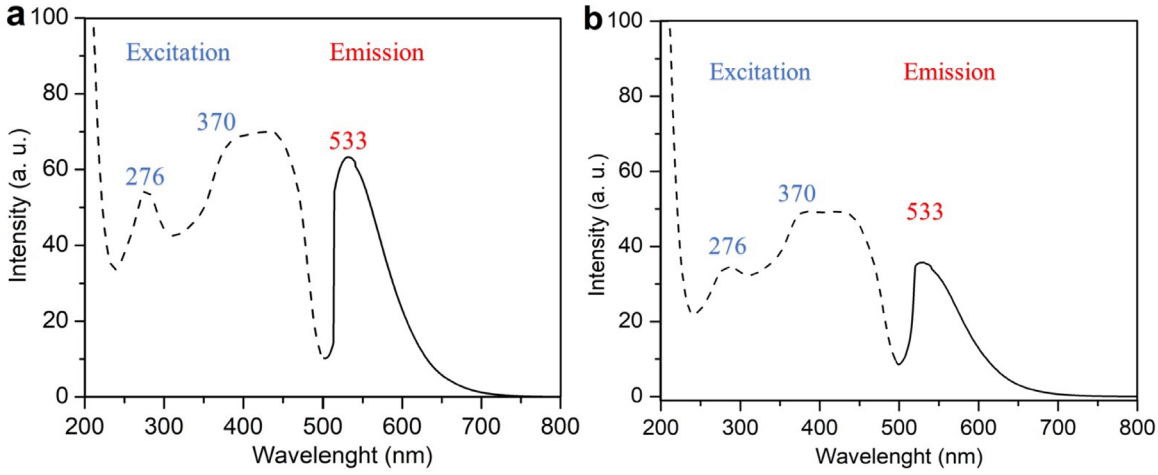

Figure 2: Excitation (dash line) and emission (straight line) spectrum of (a) ligand **NH** and (b) hybrid material **SBA-15/APTES-NH**.

due to the absence of chromophore groups. By excitation at 276 and 370 nm for the ligand **NH**, it gave emission peaks centered at 308 and 533 nm from respective isatin and thiophene chromophores [47,50]. By using the same excitation peaks, the monitoring spectrum for the hybrid materials showed the same narrow and intense emission peak. Such small decrease in the emission intensity in the hybrid material can be observed due to the degree of loading for the organic moieties not only onto the surface but also in the silicate channels as found in many reports of functionalization mesoporous silica with functional groups [51].

The sensing properties of **SBA-15/APTES-NH** were conducted by the solid method. Solid methods or solid-contact have major advantages such as minimizing waste from organic solvents when compared to chemosensors which were used as organic solvents such as dimethylsulfoxide and acetonitrile [52,53]. Besides that, the organic solvent can interfere with the sensing process and change the responsive optical properties of certain chemosensors [54]. Figure 3 shows that the changes in excitation and emission properties of hybrid material **SBA-15/APTES-NH** after getting mixed with the solution of 100 mM metal ions (Ca^{2+}, Co^{2+}, Cu^{2+}, Fe^{3+}, K^{+}, Mg^{2+}, Mn^{2+}, and Zn^{2+}). By using the same excitation for monitoring emission properties of the hybrid material, it was found that the **SBA-15/APTES-NH** showed a decrease in its emission intensities for Fe^{3+} in 77% (Figure 3a) and 84% (Figure 3b) at 276 and 374 nm. In this case, DI/I_0 described as the sensing capability of the host (**SBA-15/APTES-NH**) for sensing same guest (metal ions) [25,55] where the value ΔI is $I\text{-}I_0$, (I_0 is the fluorescent intensity for the only composite **SBA-15/APTES-NH** while I is the fluorescent intensity for the sensor with metal ions). As can be seen in Figure 4a, the largest $\Delta I/I_0$ (approximately 0.84) is observed in the presence of Fe^{3+}, whereas a small change was observed in the presence of other metal ions. Thus, hybrid material **SBA-15/APTES-NH** shows a remarkable sensitivity for the fluorescent chemosensor of Fe^{3+} ions.

Interestingly, as shown in Figure 4a, the **SBA-15/APTES-NH** showed the second highest in the decrease of emission intensity for sensing Cu^{2+} ions in 33% and 45% upon monitoring at 276 and 370 nm. Such sensing capability is almost half of the performance in the detection of Fe^{3+}. Of interest to the real sample, the **SBA-15/APTES-NH** was used to detect the mixture of both ions with the same concentration (100 mM) in order to evaluate the selectivity and/or interference. Since the decrease of the emission intensity is between the response of the hybrid chemosensor for sensing sample containing Cu^{2+} and Fe^{3+} ions, the presence of Cu^{2+} ions in the mixture was found to reduce the performance of the hybrid material around 7% only in the detection of Fe^{3+} ions (as shown in Figure 4b). From this finding, it can also be concluded that the hybrid chemosensor is more selective to detect Fe^{3+} than Cu^{2+} ions with only small interference to the presence of Cu^{2+} ions.

The sensing capability of **SBA-15/APTES-NH** was studied by addition of various concentrations of Fe^{3+} ions in the range of 50-200 mM. Figure 5a and 5b shows the changes in the emission intensities of **SBA-15/APTES-NH** upon monitoring at excitation wavelengths of 276 and 370 nm. From that evaluation, the chemosensor showed gradually quenching of its emission intensity with an increasing concentration of Fe^{3+} ions up to 200 mM. Moreover, the Stern-Volmer plot (as shown in Figure 5c) with a variation of the concentration indicates that the

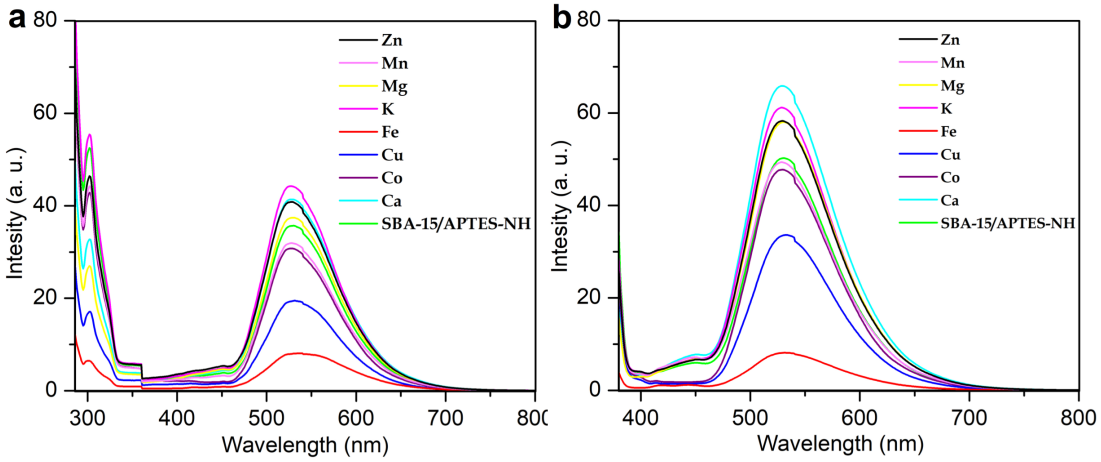

Figure 3: Emission spectral changes of the hybrid material **SBA-15/APTES-NH** with excitation wavelengths at (a) 276 and (b) 370 nm after sensing various metal ions.

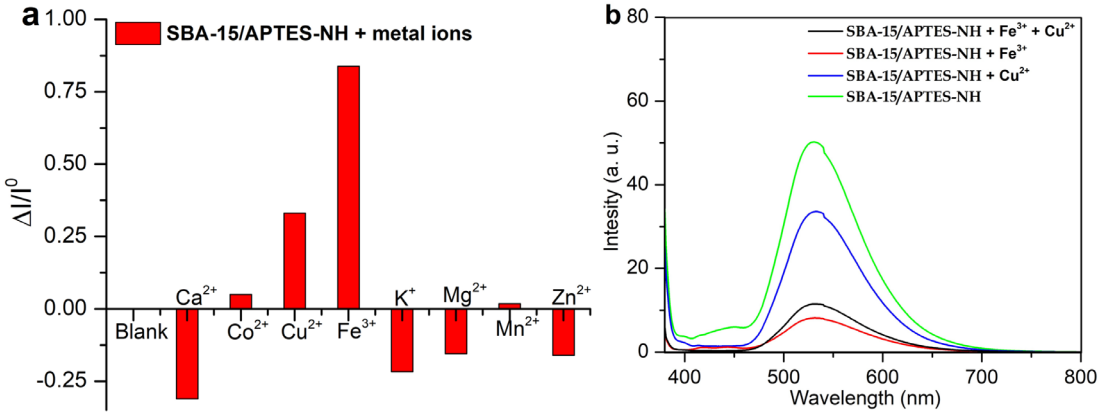

Figure 4: (a) Sensing capability (DI/I_0) of **SBA-15/APTES-NH** for the detection of various metal ions and (b) changes in emission intensity in the presence of a mixture of Fe^{3+} and Cu^{2+} in an equal concentration of 100 mM with an excitation at 370 nm.

changes in emission intensities upon detection of the Fe^{3+} ions are linearly dependent on the increase in the concentration of the guest for both excitation wavelengths. Such changes can be identified as dynamical interaction of the sensing site toward the presence of Fe^{3+} ions. The limit of detection (LOD) of **SBA-15/APTES-NH** can be calculated with the equation LOD = 3 SD/K_{sv} [56,57], where SD is the standard deviation of the blank signals and K_{sv} is the quenching constant of Stern-Volmer. The result of SD and K_{sv} is 0.006905426 and 0.0139 mM^{-1}, respectively. Therefore, the detection limit of **SBA-15/APTES-NH** is 1.49 mM, which indicates that the **SBA-15/APTES-NH** is potentially used for detection of Fe^{3+} ions even in the lower concentration. Otherwise, the **SBA-15/APTES-NH** sensor can be potentially applied to detect Fe^{3+} ions in the environmental and pharmaceutical fields [58,59]. Moreover, limit of quantification (LOQ) can be also calculated with the equation of LOQ = 10 SD/K_{sv} [60]. The LOQ value of **SBA-15/APTES-NH** is 6.32 mM. By using the calibration curve as the relative emission intensity of **SBA-15/APTES-NH** at 533 nm versus Fe^{3+} concentration, the quantitative analysis can be performed in the presence of real samples. In the linear range between 50 to 200 mM, the calibration curve is not straightforward with a high relative coefficient due to the inhomegenous distribution of organic moieties in the grafting with **SBA-15/APTES**. Such drawback in the loading of organic functional groups has been discussed in many reports [52]. Of interest, the good reproducibility of **SBA-15/APTES-NH** was shown with the small RSD value in 2.7 and 7.4% for both excitation wavelengths of 276 and 370 nm (Figure 5d).

Reusability testing is important factors for the development of novel chemosensors in practical applications. Previously, chemosensors for the detection

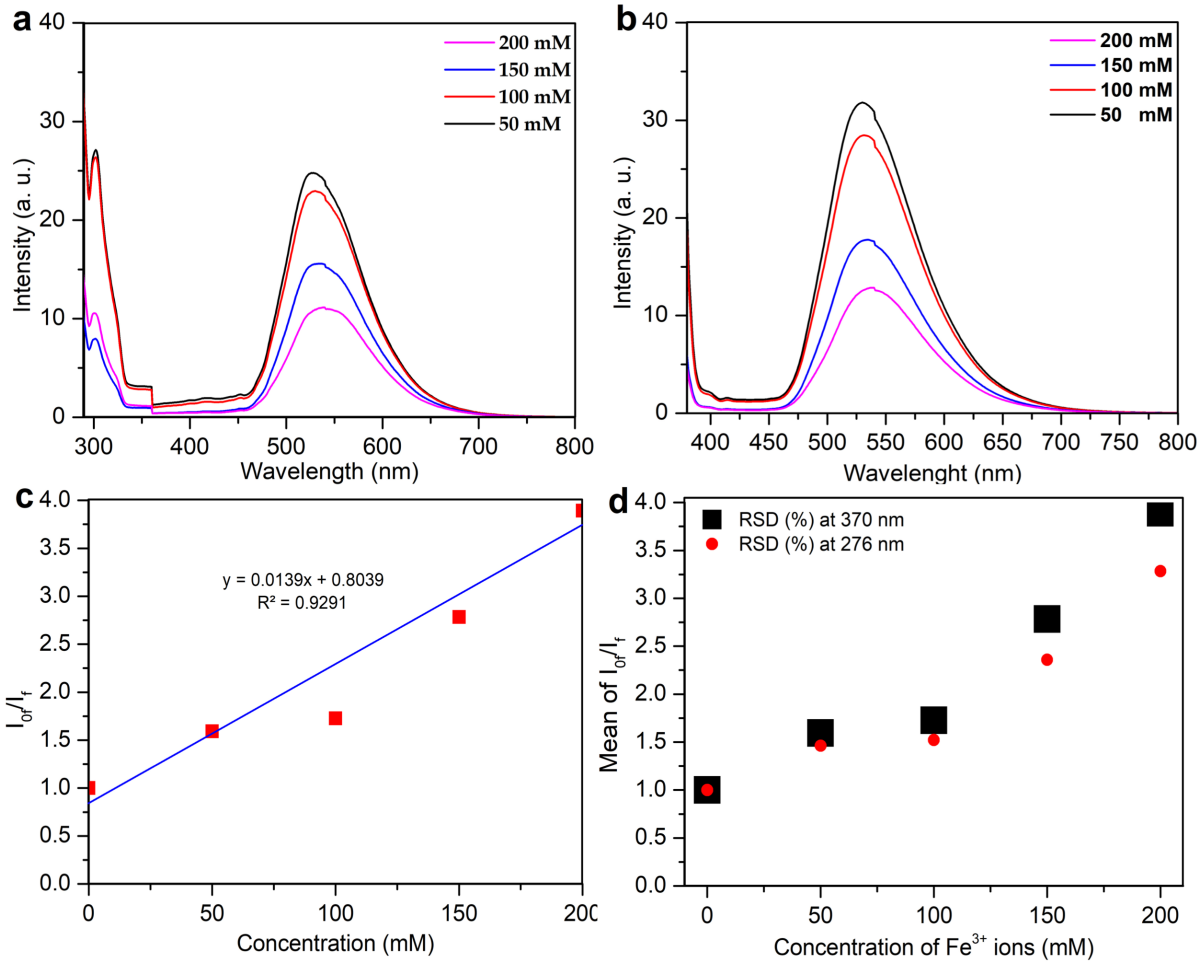

Figure 5: Effect of Fe^{3+} concentrations on the emission spectra changes of **SBA-15/APTES-NH** at (a) 276 and (b) 370 nm and (c) Stern-Volmer plot (wavelength excitation at 370 nm) between relative emission intensity at 533 nm as well as (d) changes in emission intensity with variation concentration of Fe^{3+} ions at 276 and 370 nm with SD error bars.

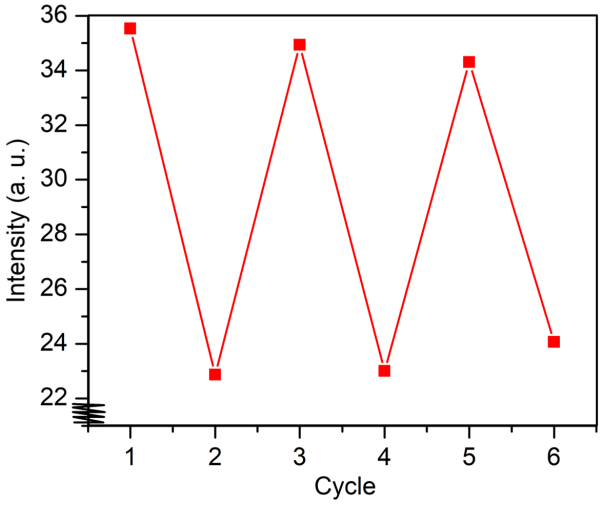

Figure 6: Reversibility testing with changes in fluorescent intensity of **SBA-15/APTES-NH** at 533 nm upon addition to KSCN in HCl solution.

of Fe^{3+} ions based on functionalized **SBA-15** have not yet reported the reversibility testing [44,61]. In this study, the reversibility of the Fe^{3+} was treated by the addition of the binding agent of potassium thiocyanate (KSCN) in hydrochloric acid (HCl) (pH = 1) to the hybrid chemosensor consisting of Fe^{3+} ions. The testing was performed until the color of the solution of KSCN in HCl changes from red to a colorless solution. As shown in Figure 6, the hybrid chemosensor can be recycled up to three times with only a small decrease in the performance. Such reusability result is an important achievement for the fabrication of Fe^{3+} fluorescent chemosensors.

The FT-IR spectrum of the **SBA-15/APTES-NH** with the absence and presence of Fe^{3+} ions was particularly analyzed in the range of 1800-400 cm^{-1} using ATR (Figure 7a). The FT-IR spectrum of **SBA-15/APTES-NH** shows characteristic vibration peaks at 1707, 1662, 1341 and 751 cm^{-1}, which are assigned to the vibrations of carbonyl amide,

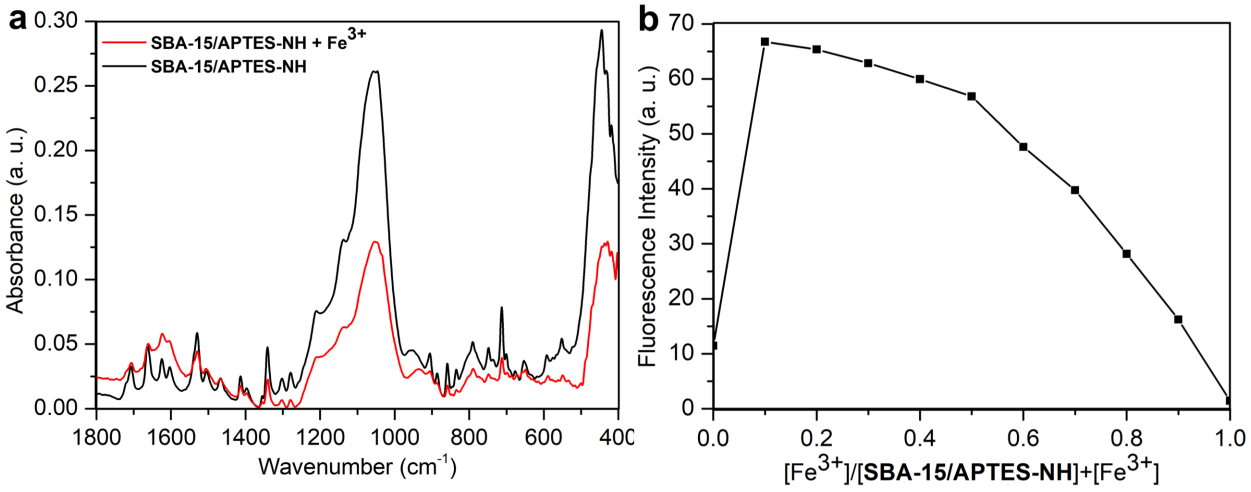

Figure 7: (a) FT-IR spectrum of the **SBA-15/APTES-NH** with the absence and presence of Fe^{3+} ions and (b) Job's plot for Fe^{3+} ions versus nett volume of ligand **NH** to Fe^{3+} ion.

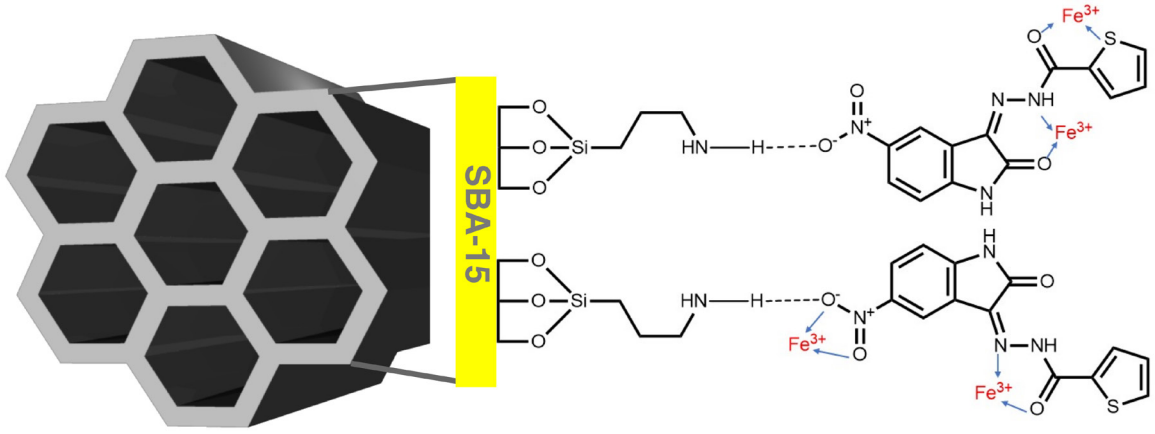

Figure 8: Proposed plausible mechanism for the interaction of ligand **NH** as the sensing site in the hybrid material **SBA-15/APTES-NH** for the detection of Fe^{3+} ions.

C=N, C-N and C-S groups, respectively. Moreover, the vibration peak of N-H bending from isatin ring, Schiff base, and aminopropyl (from **APTES**) groups were observed at 1624, 1603, and 1530 cm^{-1}. Upon addition of Fe^{3+} ions to the chemosensor, the N-H bending of Schiff base and C=O peaks slightly shifted with small changes in their intensities from 1707 to 1706 cm^{-1}, 1603 to 1605 cm^{-1} and 1530 to 1529 cm^{-1}. In shall be noted that the vibration peak of the N-H from Schiff base was increased in 1.25 times of its intensity while vibration peak for C=N was broadened and vibration peaks for C-N and C-S were reduced significantly. Such changes clearly suggest that Fe^{3+} ions have formed strong interactions with the Schiff base and thiophene ring while a weak interaction can also be possible with aminopropyl-bridged nitro isatin group [53]. Further analysis with Job's plot for binding analysis of the ligand **NH** to Fe^{3+} ions in the solution phase as shown in Figure 7b confirmed that the interaction were initially closed to 1:1 of Fe^{3+} ions to ligand **NH** and then gradually changed to 1:4 to form the stable binding interactions. Based on the above finding, the interactions of Fe^{3+} ions with the sensing site of hybrid material **SBA-15/APTES-NH** can be proposed as shown in Figure 8.

4 Conclusion

The organic-inorganic hybrid **SBA-15/APTES-NH** was synthesized and characterized using the mesoporous silica **SBA-15** and the new nitroisatin (ligand **NH**). This

hybrid **SBA-15/APTES-NH** was successfully applied as a chemosensor and showed a good sensing capability towards Fe^{3+} ions from its emission changes at 533 nm with an quenching phenomenon up to 84%, low LOD, and RSD as well as high reusability. From the Stern-Volmer diagram, the **SBA-15/APTES-NH** showed a linear graphic with the excitation of wavelengths at 276 and 370 nm for a good relationship of the emission changes with the increasing concentration of Fe^{3+} ions. All of the obtained results suggest that the new hybrid material **SBA-15/APTES-NH** with an intense and narrow emission peak is a potential fluorescent chemosensor for the detection of Fe^{3+} ions.

Acknowledgment: The authors thank Ministry of Research, Technology and Higher Education, The Republic of Indonesia for financial support through Higher Education Excellent Applied Research Grant (Penelitian Terapan Unggulan Perguruan Tinggi) 2019 with Agreement No. 006/MACHUNG/LPPM/SP2H-LIT-MULTI/III/2019. This research was partially financed by COMSTECH-TWAS Joint Research Grants Programme with a contract agreement number of 17-139RG/MSN/AS_C-FR3240300067.

Conflict of interest: Authors declare no conflict of interest.

References

[1] Li B., Tian J., Zhang D., Tian F., A novel colorimetric fluorescence sensor for Fe^{3+} based on quinoline Schiff base. Luminescence, 2017, 32, 1567–1573, doi:10.1002/bio.3361.

[2] Karimi M., Badiei A., Ziarani G.M., A novel naphthalene-immobilized nanoporous sba-15 as a highly selective optical sensor for detection of Fe^{3+} in water. J. Fluoresc., 2015, 25, 1297–1302, doi:10.1007/s10895-015-1617-y.

[3] Lashgari N., Badiei A., Ziarani G.M., Modification of mesoporous silica SBA-15 with different organic molecules to gain chemical sensors : a review organic molecules and its role. Nano. Chem. Res., 2016, 1, 127–141, doi:10.7508/ncr.2016.01.014.

[4] Zhao L., Li J., Sui D., Wang Y., Highly selective fluorescence chemosensors based on functionalized SBA-15 for detection of Ag^{+} in aqueous media. Sensor. Actuators B Chem., 2017, 242, 1043–1049, doi:10.1016/j.snb.2016.09.148.

[5] Ni J., Li B., Zhang L., Zhao H., Jiang H., A fluorescence turn-on probe based on rhodamine derivative and its functionalized silica material for Hg^{2+} selective detection. Sensor. Actuators B Chem., 2015, 215, 174–180, doi:10.1016/j.snb.2015.03.057.

[6] Pan C., Wang K., Ji S., Wang H., Li Z., He H., et al., Schiff base derived Fe^{3+} selective fluorescence turn-off chemsensors based on triphenylamine and indole: Synthesis, properties and application in living cells. RSC Adv., 2017, 7, 36007–36014, doi:10.1039/c7ra05064j.

[7] Neupane L.N., Park J.Y., Park J.H., Lee K.H., Turn-on fluorescent chemosensor based on an amino acid for Pb (II) and Hg (II) ions in aqueous solutions and role of tryptophan for sensing. Org. Lett., 2013, 15, 254–257, doi:10.1021/ol3029516.

[8] Li H.G., Yang Z.Y., Qin D.D., A new Schiff-base type selective fluorescent chemosensor for Cu^{2+}. Inorg. Chem. Commun., 2009, 12, 494–497, doi:10.1016/j.inoche.2009.04.003.

[9] He Y., Yin J., Wang G., New selective "on-off" fluorescence chemosensor based on carbazole Schiff base for Fe^{3+} detection. Chem. Heterocycl. Compd., 2018, 54, 146–152, doi:10.1007/s10593-018-2246-6.

[10] Horak E., Vianello R., Hranjec M., Steinberg I.M., Colourimetric and fluorimetric metal ion chemosensor based on a benzimidazole functionalised Schiff base. Supramol. Chem., 2018, 0278, 1–10, doi:10.1080/10610278.2018.1436708.

[11] Mureseanu M., Reiss A., Stefanescu I., David E., Parvulescu V., Renard G., et al., Modified SBA-15 mesoporous silica for heavy metal ions remediation. Chemosphere, 2008, 73, 1499–1504, doi:10.1016/j.chemosphere.2008.07.039.

[12] Singh T.S., Paul P.C., Pramanik H.A.R., Fluorescent chemosensor based on sensitive Schiff base for selective detection of Zn^{2+}. Spectrochim. Acta A Mol. Biomol. Spectrosc., 2014, 121, 520–526, doi:10.1016/j.saa.2013.11.002.

[13] Mahale R.G., Nagarale D.V., Schiff Base : Multidisciplinary tool in chemistry. Eur. J. Pharm. Med. Res., 2017, 4, 193–201.

[14] Kim M.S., Lee S.Y., Jung J.M., Kim C., A new Schiff-base chemosensor for selective detection of Cu^{2+} and Co^{2+} and its copper complex for colorimetric sensing of S^{2-} in aqueous solution. Photochem. Photobiol. Sci., 2017, 16, 1677–1689, doi:10.1039/C7PP00229G.

[15] Cigáň M., Jakusová K., Donovalová J., Szöcs V., Gáplovský A., Isatin *N*-phenylsemicarbazone: Effect of substituents and concentration on anion sensing selectivity and sensitivity. RSC Adv., 2014, 4, 54072–54079, doi:10.1039/c4ra04847d.

[16] Goswami S., Paul S., Manna A., Selective "naked eye" detection of Al (III) and PPi in aqueous media on a rhodamine-isatin hybrid moiety. RSC Adv., 2013, 3, 10639–10643, doi:10.1039/c3ra40984h.

[17] Kundu A., Pathak S., Pramanik A., Synthesis and fluorescence properties of isatin-based spiro compounds: switch off chemosensing of copper (II) ions. Asian J. Org. Chem., 2013, 2, 869–876, doi:10.1002/ajoc.201300153.

[18] Mahajan P.G., Bhopate D.P., Kolekar G.B., Patil S.R., *N*-methyl isatin nanoparticles as a novel probe for selective detection of Cd^{2+} ion in aqueous medium based on chelation enhanced fluorescence and application to environmental sample. Sensor. Actuat. B Chem., 2015, 220, 864–872, doi:10.1016/j.snb.2015.05.119.

[19] Bardajee G.R., Hooshyar Z., Shahidi F.E., Synthesis and characterization of a novel Schiff-base/SBA-15 nanoadsorbent for removal of methylene blue from aqueous solutions. Int. J. Environ. Sci. Technol., 2015, 12, 1737–1748, doi:10.1007/s13762-014-0732-7.

[20] Sevimli F., Yilmaz A., Surface functionalization of SBA-15 particles for amoxicillin delivery. Microporous Mesoporous Mater., 2012, 158, 281–291, doi:10.1016/j.micromeso.2012.02.037.

[21] Zhang J.J., Cheng F.F., Li J.J., Zhu J.J., Lu Y., Fluorescent nanoprobes for sensing and imaging of metal ions: Recent advances and future perspectives. Nano Today, 2016, 11, 309–329, doi:10.1016/j.nantod.2016.05.010.
[22] Zhang J., Zhu J., A novel amperometric biosensor based on gold nanoparticles-mesoporous silica composite for biosensing glucose. Sci. China, Ser. B Chem., 2009, 52, 815–820, doi:10.1007/s11426-009-0079-y.
[23] Tahmasbi L., Sedaghat T., Motamedi H., Kooti M., Mesoporous silica nanoparticles supported copper (II) and nickel (II) Schiff base complexes: Synthesis, characterization, antibacterial activity and enzyme immobilization. J. Solid State Chem., 2018, 258, 517–525, doi:10.1016/j.jssc.2017.11.015.
[24] Badiei A., Razavi B.V., Goldooz H., Ziarani G.M., Faridbod F., Ganjali M.R., A novel fluorescent chemosensor assembled with 2,6-bis(2-benzimidazolyl)pyridine-functionalized nanoporous silica-type SBA-15 for recognition of Hg^{2+} ion in aqueous Media. Int. J. Environ. Res., 2018, 12, 109–115, doi:10.1007/s41742-018-0075-1.
[25] Zhao L., Sui D., Wang Y., Fluorescence chemosensors based on functionalized SBA-15 for detection of Pb^{2+} in aqueous media. RSC Adv., 2015, 5, 16611–16617, doi:10.1039/c5ra00696a.
[26] Dolatyari L., Yaftian M.R., Rostamnia S., Removal of uranium (VI) ions from aqueous solutions using Schiff base functionalized SBA-15 mesoporous silica materials. J. Environ. Manage., 2016, 169, 8–17, doi:10.1016/j.jenvman.2015.12.005.
[27] Gupta V.K., Ganjali M.R., Norouzi P., Khani H., Nayak A., Agarwal S., Electrochemical analysis of some toxic metals by ion-selective electrodes. Crit. Rev. Anal. Chem., 2011, 41, 282–313, doi:10.1080/10408347.2011.589773.
[28] Lintang H.O., Kinbara K., Yamashita T., Aida T., Metal-ion permeation in congested nanochannels: The exposure effect of Ag^{+} ions on the phosphorescent properties of a gold (I)-pyrazolate complex that is confined in the nanoscopic channels of mesoporous silica. Chem. Asian J., 2012, 7, 2068–2072, doi:10.1002/asia.201200041.
[29] Gupta V.K., Singh A.K., Kumawat L.K., Thiazole Schiff base turn-on fluorescent chemosensor for Al^{3+} ion. Sensor. Actuat. B Chem., 2014, 195, 98–108, doi:10.1016/j.snb.2013.12.092.
[30] Gupta V.K., Kumar S., Singh R., Singh L.P., Shoora S.K., Sethi B., Cadmium (II) ion sensing through p-tert-butyl calix[6]arene based potentiometric sensor. J. Mol. Liq., 2014, 196, 65–68, doi:10.1016/j.molliq.2014.02.001.
[31] Gupta V.K., Mergu N., Kumawat L.K., Singh A.K., Selective naked-eye detection of Magnesium (II) ions using a coumarin-derived fluorescent probe. Sensor. Actuators B Chem., 2015, 207, 216–223, doi:10.1016/j.snb.2014.10.044.
[32] Gupta V.K., Mergu N., Kumawat L.K., Singh A.K., A reversible fluorescence "off-on-off" sensor for sequential detection of aluminum and acetate/fluoride ions. Talanta, 2015, 144, 80–89, doi:10.1016/j.talanta.2015.05.053.
[33] Karimi-Maleh H., Tahernejad-Javazmi F., Atar N., Yola M.L., Gupta V.K., Ensafi A.A., A Novel DNA biosensor based on a pencil graphite electrode modified with polypyrrole/functionalized multiwalled carbon nanotubes for determination of 6-mercaptopurine anticancer drug. Ind. Eng. Chem. Res., 2015, 54, 3634–3639, doi:10.1021/ie504438z.
[34] Hartmann M., Vinu A., Mechanical stability and porosity analysis of large-pore SBA-15 mesoporous molecular sieves by mercury porosimetry and organics adsorption. Langmuir, 2002, 18, 8010–8016, doi:10.1021/la025782j.
[35] Karimi M., Badieia A., Ziarani G.M., Fluorescence-enhanced optical sensor for detection of Al^{3+} in water based on functionalised nanoporous silica type SBA-15. Chem. Pap., 2016, 70, 1431–1438, doi:10.1515/chempap-2016-0079.
[36] Lashgari N., Badiei A., Ziarani G.M. Selective detection of Hg^{2+} ion in aqueous medium with the use of 3-(pyrimidin-2-ylimino) indolin-2-one-functionalized SBA-15. Appl. Organomet. Chem., 2018, 32, 1–8, doi:10.1002/aoc.3991.
[37] Wang J., Chu S., Kong F., Luo L., Wang Y., Zou Z., Designing a smart fluorescence chemosensor within the tailored channel of mesoporous material for sensitively monitoring toxic heavy metal ions Pb (II). Sensor. Actuat. B Chem., 2010, 150, 25–35, doi:10.1016/j.snb.2010.07.050.
[38] Gao L., Wang Y., Wang J., Huang L., Shi L., Fan X., et al., A novel Zn^{II}-sensitive fluorescent chemosensor assembled within aminopropyl-functionalized mesoporous SBA-15. Inorg. Chem., 2006, 45, 6844–6850, doi:10.1021/ic0516562.
[39] Zhang H., Zhang P., Ye K., Sun Y., Jiang S., Wang Y., et al., Mesoporous material grafted with luminescent molecules for the design of selective metal ion chemosensor. J. Lumin., 2006, 117, 68–74, doi:10.1016/j.jlumin.2005.04.009.
[40] Shamel A., Salemnush T., Synthesis and fluorescence study of the grafted salicylidene Schiff base onto SBA-15 mesoporous silica for detecting Zn^{2+} traces in aqueous medium. Russ. J. Appl. Chem., 2016, 89, 500–504, doi:10.14423/SMJ.0000000000000193.
[41] Liu S., Wang Y.M., Han J., Fluorescent chemosensors for copper (II) ion: Structure, mechanism and application. J. Photochem. Photobiol. C Photochem. Rev., 2017, 32, 78–103, doi:10.1016/j.jphotochemrev.2017.06.002.
[42] Chen X., Yamaguchi A., Namekawa M., Kamijo T., Teramae N., Tong A., Functionalization of mesoporous silica membrane with a Schiff base fluorophore for Cu (II) ion sensing. Anal. Chim. Acta, 2011, 696, 94–100, doi:10.1016/j.aca.2011.04.002.
[43] Huang J., Ye M., Chen R., He Q.Z., Salicylidene Schiff Base Assembled with Mesoporous Silica SBA-15 for Cu (II) Removal in Aqueous Media. Adv. Mater. Res., 2011, 356–360, 373–381, doi:10.4028/www.scientific.net/AMR.356-360.373.
[44] Wang J.Q., Huang L., Xue M., Wang Y., Gao L., Zhu J.H., et al., Architecture of a hybrid mesoporous chemosensor for Fe^{3+} by covalent coupling bis-schiff base PMBA onto the CPTES-functionalized SBA-15. J. Phys. Chem. C, 2008, 112, 5014–5022, doi:10.1021/jp7099948.
[45] Afshani J., Badiei A., Lashgari N., Ziarani G.M., A simple nanoporous silica-based dual mode optical sensor for detection of multiple analytes (Fe^{3+} , Al^{3+} and CN^{-}) in water mimicking XOR logic gate. RSC Adv., 2016, 6, 5957–5964, doi:10.1039/C5RA23136A.
[46] Lashgari N., Badiei A., Ziarani G.M., A novel functionalized nanoporous SBA-15 as a selective fluorescent sensor for the detection of multianalytes (Fe^{3+} and $Cr_2O_7^{2-}$) in water. J. Phys. Chem. Solids, 2017, 103, 238–248, doi:10.1016/j.jpcs.2016.11.021.
[47] Tiwari K., Mishra M., Singh V.P., A highly sensitive and selective fluorescent sensor for Al^{3+} ions based on thiophene-2-carboxylic acid hydrazide Schiff base. RSC Adv., 2013, 3, 12124–12132, doi:10.1039/c3ra41573b.

[48] Roslan N., Lintang H.O., Endud S., Bakar M.B., Ramli Z., Synthesis of mesoporous SBA-15/ionic liquid nanocomposites for the selective oxidation of 2,3,6-trimethylphenol. Malaysian J. Catal., 2016, 1, 27–31.
[49] Fahmi M.R.G., Khumaidah L., Ilmiah T.K., Fadlan A., Santoso M., 2-Thiophenecarboxylic acid hydrazide derivatives: synthesis and anti-tuberculosis studies. IOP Conf. Ser. Mater. Sci. Eng., 2018, 349, 012039, doi:10.1088/1757-899X/349/1/012039.
[50] Lashgari N., Badiei A., Ziarani G.M., Faridbod F., Isatin functionalized nanoporous SBA-15 as a selective fluorescent probe for the detection of Hg (II) in water. Anal. Bioanal. Chem., 2017, 409, 3175–3185, doi:10.1007/s00216-017-0258-1.
[51] Hoffmann F., Cornelius M., Morell J., Fröba M., Silica-based mesoporous organic-inorganic hybrid materials. Angew. Chem. Int. Ed., 2006, 45, 3216–3251, doi:10.1002/anie.200503075.
[52] Zhu W., Yang L., Fang M., Wu Z., Zhang Q., Yin F., et al., New carbazole-based Schiff base: Colorimetric chemosensor for Fe^{3+} and fluorescent turn-on chemosensor for Fe^{3+} and Cr^{3+}. J. Lumin., 2015, 158, 38–43, doi:10.1016/j.jlumin.2014.09.020.
[53] Zhang S., Sun T., Xiao D., Yuan F., Li T., Wang E., et al., A dual-responsive colorimetric and fluorescent chemosensor based on diketopyrrolopyrrole derivative for naked-eye detection of Fe^{3+} and its practical application. Spectrochim. Acta A Mol. Biomol. Spectrosc., 2018, 189, 594–600, doi:10.1016/j.saa.2017.09.001.
[54] Huang X., Miao Q., Wang L., Jiao J., He X., Cheng Y., A highly sensitive and selective fluorescence chemosensor for Cu^{2+} and Zn^{2+} based on solvent effect. Chinese J. Chem., 2013, 31, 195–199, doi:10.1002/cjoc.201200619.
[55] Narita M., Hamada F., Suzuki I., Osa T., Variations of fluorescent molecular sensing for organic guests by regioselective anthranilate modified β- and γ-cyclodextrins. J. Chem. Soc. Perkin Trans. 2, 1998, 0, 2751–2758, doi:10.1039/a802955e.
[56] Committee A.M., Recommendations for the definition, estimation and use of the detection limit. Analyst, 1987, 112, 199–204, doi:10.1039/AN9871200199.
[57] Alim N.S., Lintang H.O., Yuliati L., Fabricated metal-free carbon nitride characterizations for fluorescence chemical sensor of nitrate ions. J. Teknol., 2015, 13, 1–6, doi:10.11113/jt.v76.5812.
[58] Dongare P.R., Gore A.H., Kondekar U.R., Kolekar G.B., Ajalkar B.D., A Quinazolinone based fluorescent chemosensor for selective detection of Fe (III) in aqueous media: Applications to pharmaceutical and environmental analysis. Inorg. Nano-Metal Chem., 2018, 48, 49–56, doi:10.1080/24701556.2017.1357631.
[59] Nayab P.S., Shkir M., Gull P., AlFaify S., A highly sensitive "Off-On" optical and fluorescent chemodosimeter for detecting iron (III) and its application in practical samples: An investigation of Fe^{3+} induced oxidation by mass spectrometry. J. Photochem. Photobiol. A, 2017, 347, 209–217, doi:10.1016/j.jphotochem.2017.07.048.
[60] Shrivastava A., Gupta V.B., Methods for the determination of limit of detection and limit of quantitation of the analytical methods. Chronicles Young Sci., 2011, 2, 21–25, doi:10.4103/2229-5186.79345.
[61] Yadavi M., Badiei A., Ziarani G.M., A novel Fe^{3+} ions chemosensor by covalent coupling fluorene onto the mono, di- and tri-ammonium functionalized nanoporous silica type SBA-15. Appl. Surf. Sci., 2013, 279, 121–128, doi:10.1016/j.apsusc.2013.04.048.